



PAPER • OPEN ACCESS

40 Hz steady-state visually evoked potentials recovered during oscillating transcranial electrical stimulation

To cite this article: Laura Hainke et al 2025 Biomed. Phys. Eng. Express 11 055031

View the article online for updates and enhancements.

You may also like

- Photonic-digital hybrid artificial intelligence hardware architectures: at the interface of the real and virtual worlds
 Lília M S Dias, Dinis O Abranches, Ana R Bastos et al.
- Fractal analysis for cognitive impairment classification in DAVF using machine learning Jithin Sivan Sulaja, Santhosh Kumar Kannath, Ramshekhar N Menon et al.
- Global evidence that cold rocky landforms support icy springs in warming mountains Stefano Brighenti, Constance I Millar, Scott Hotaling et al.

Biomedical Physics & Engineering Express



OPEN ACCESS

RECEIVED

24 July 2025

REVISED

6 August 2025

ACCEPTED FOR PUBLICATION

21 August 2025

PUBLISHE

8 September 2025

Original content from this work may be used under the terms of the Creative Commons Attribution 4.0 licence.

Any further distribution of this work must maintain attribution to the author(s) and the title of the work, journal citation and DOI.



PAPER

40 Hz steady-state visually evoked potentials recovered during oscillating transcranial electrical stimulation

Laura Hainke^{1,2,3,*}, Manuel Spitschan^{2,4,5}, Josef Priller^{1,6,7,8}, Paul Taylor^{3,9} and James Dowsett^{3,10}

- Department of Psychiatry and Psychotherapy, TUM School of Medicine and Health, Technical University of Munich, Ismaninger Str. 22, 81675 Munich, Germany
- Department of Health and Sport Sciences, TUM School of Medicine and Health, Technical University of Munich, Am Olympiacampus 11, 80809 Munich, Germany
- ³ Department of Psychology, LMU Munich, Leopoldstr. 13, 80802 Munich, Germany
- ⁴ Translational Sensory & Circadian Neuroscience, Max Planck Institute for Biological Cybernetics, Max-Planck-Ring 8, 72076 Tübingen, Germany
- ⁵ TUM Institute of Advanced Study (TUM-IAS), Technical University of Munich, Garching, Lichtenbergstraße 2a, 85748 Garching bei München, Germany
- Neuropsychiatry, Charité—Universitätsmedizin Berlin and DZNE, Charitépl. 1, 10117 Berlin, Germany
- University of Edinburgh and UK DRI, Edinburgh, Old College, South Bridge, Edinburgh EH8 9YL, United Kingdom
- ⁸ German Center for Mental Health (DZPG), Munich, Virchowweg 23, 10117 Berlin, Germany
- ⁹ Department of Psychology, University of Zurich, Binzmuehlestrasse 14, 8050 Zurich, Switzerland
- $^{10}\ Division\ of\ Psychology,\ University\ of\ Stirling,\ Stirling,\ FK9\ 4LA,\ Scotland,\ United\ Kingdom$
- * Author to whom any correspondence should be addressed.

E-mail: laura.hainke@tum.de, manuel.spitschan@tum.de, josef.priller@tum.de, paul.taylor@psychologie.uzh.ch and james.dowsett@stir.ac.uk

Keywords: transcranial electrical stimulation, steady-state visually evoked potential (SSVEP), electroencephalography (EEG), gamma, flicker, multimodal, non-invasive brain stimulation

Supplementary material for this article is available online

Abstract

Background. Combining Transcranial Electrical Stimulation and Visual Stimulation at the gamma frequency of 40 Hz holds scientific and clinical potential, but requires concurrent electrophysiological measurement to quantify neuronal effects. This poses substantial methodological challenges: electrical stimulation artifacts largely overshadow EEG signals; gamma signals' amplitude is particularly low; and oculo-muscular confounds overlap in frequency. With appropriate artifact removal, we aimed to record 40 Hz Steady-State Visually Evoked Potentials (SSVEPs) with EEG during frequency-matched electrical stimulation and explore possible interactions. Methods. In three experiments (N = 25 healthy volunteers each), we tested if electrical and visual stimulation might interact depending on which brain areas are electrically stimulated or whether the respective frequencies match—and, importantly, how effectively the data processing pipeline can separate artifacts from genuine neuronal activity. Analysing SSVEPs in the time domain, as opposed to the traditional frequency domain, enabled us to mitigate electrical artifacts flexibly through an adaptive template subtraction approach with millisecond precision. It also allowed us to extract SSVEP waveform information, in addition to amplitude. Compared to previous approaches for low frequencies, our algorithm has improved artifact template fitting, a new interpolation feature, and refined segment rejection criteria. Main Results. We successfully recovered 40 Hz SSVEPs during frequency-matched electrical stimulation applied to central and occipital regions. They closely matched baseline SSVEPs without electrical stimulation in waveform shape. A control condition (no visual stimulation, only electrical) produced uncorrelated low-amplitude signals, further demonstrating robust artifact removal. No interactions between electrical and visual stimulation were found. Significance. We demonstrated how 40 Hz SSVEPs can be reliably measured with EEG during frequency-matched electrical brain stimulation, distinguishing neuronal activity from electrical or physiological confounds. This method now enables fundamental and clinical researchers to combine

rhythmic sensory and electrical stimulation in the gamma band and concurrently quantify neuronal electrophysiological effects.

Abbreviations

EEG	Electroencephalography
SSVEP	Steady-State Visually Evoked Potential
VS	Visual Stimulation
TES	Transcranial Electric Stimulation
tDCS	Transcranial Direct Current Stimulation
tACS	Transcranial Alternating Current Stimulation
FFT	Fast-Fourier Transform
ATS	Adaptive Template Subtraction

1. Introduction

Visual Stimulation (VS) and Transcranial Electrical Stimulation (TES) can be applied rhythmically to safely and effectively modulate neuronal oscillations. Oscillations in the gamma band (30-100 Hz, especially 40 Hz) are of particular interest due to their role in perception and memory (Herrmann et al 2010) and because they are disrupted in disorders such as Alzheimer's Disease (Güntekin et al 2022). By modulating gamma activity, both VS and TES are promising approaches to causally investigate related cognitive functions (Hanslmayr et al 2019) and to intervene against cognitive decline (Strüber and Herrmann 2020, Traikapi and Konstantinou 2021, Guan et al 2022, Nissim et al 2023, Shu et al 2024). Since audiovisual stimulation yields larger effects than visual alone (Blanco-Duque et al 2023), combining visual and electrical stimulation could also enhance effects, but this approach is untested. Importantly, neuronal responses need to be measured during stimulation, as the modulation of neuronal activity is necessary for studying gamma-related cognitive functions (Hanslmayr et al 2019) and for clinical effects (Blanco-Duque et al 2023).

Mechanistically, rhythmic VS elicits oscillatory brain activity measurable as Steady-State Visually Evoked Potentials (SSVEPs), particularly in the visual cortex (Herrmann 2001, Bayram *et al* 2011). In contrast, rhythmic TES—in the form of Transcranial Alternating Current Stimulation (tACS) or pulsed Transcranial Direct Current Stimulation (tDCS)—modulates cortical excitability and entrains neural firing to the applied current (Groppa *et al* 2010, Herrmann *et al* 2013, Fröhlich 2014). We hypothesised that applying TES to the visual cortex at the same

frequency as VS could amplify visually evoked responses through resonance. However, testing this interaction requires electroencephalographic (EEG) recording during stimulation, which poses substantial challenges. First, EEG during TES is heavily contaminated by electrical artifacts that far exceed the neural signal (Bergmann et al 2016, Noury et al 2016, Kasten and Herrmann 2019). Second, visually evoked gamma activity is low in amplitude and prone to contamination by physiological artifacts—such as cranial muscle activity and microsaccades-whose frequencies are also >30 Hz and that may reflect cognitive processes (Hipp and Siegel 2013). Third, using the same frequency for both visual and electrical stimulation makes it difficult to disentangle genuine neural responses from residual artifacts.

Some previous studies have proposed strategies to mitigate TES artifacts in EEG data, although this remains challenging (Kasten and Herrmann 2019). One approach is to subtract a TES artifact template from EEG segments; outcomes are sensitive to stimulation and analysis parameters (Dowsett and Herrmann 2016). Other work reports benefits of combined TES and VS, but without concurrent EEG measurement (Somer et al 2020, Liu et al 2021, Li et al 2024), or effects of constant tDCS on low-frequency SSVEPs (Liu et al 2017, Kim et al 2019, Zhang et al 2024). To our knowledge, only a few studies have combined rhythmic VS, rhythmic TES, and concurrent electrophysiological assessments. SSVEPs have been recovered during frequency-matched TES (Haslacher et al 2021) or even enhanced by it (Ruhnau et al 2016, Dowsett et al 2020b), but only at lower frequencies <11 Hz. This avoids a frequency overlap with physiological confounds >30 Hz (Hipp and Sie-2013, Jonmohamadi and Muthukumaraswamy 2018) and takes advantage of strong endogenous alpha levels, compared to gamma. For cognition research and clinical interventions, however, 40 Hz is a crucial target (Ichim et al 2024). These neuronal frequencies are mechanistically distinct: while alpha oscillations are generated by thalamocortical loops (Hindriks and van Putten 2013), gamma oscillations require more localised cortical excitatoryinhibitory feedback loops (Buzsáki and Schomburg 2015). Overall, modulating gamma-band SSVEPs through frequency-matched TES is a timely and important subject of investigation, but measurement feasibility and interaction effects are unclear.

The present study addresses this knowledge gap. We hypothesised that it would be possible to record 40 Hz SSVEPs with EEG during electrical brain stimulation, by mitigating electrical artifacts through Adaptive Template Subtraction (ATS) and analysing

SSVEPs in the time domain akin to Event-Related Potentials. Compared to conventional frequency-domain analyses using the Fast-Fourier Transform (FFT), this approach offers several advantages such as more fine-grained artifact removal, high signal-to-noise ratio, and the possibility to inspect waveform shapes (Dowsett *et al* 2020b). We here found that our previously developed pipeline for reducing alphaband artifacts (Dowsett *et al* 2020b) did not sufficiently reduce gamma pulsed tDCS artifacts; therefore, for the current study, we optimised the algorithm, principally by improving the TES artifact templates' fit and by better dealing with persistent artifacts through interpolation and data segment rejection.

We argued based on previous research that electrical and visual stimulation might interact, which could be specific to stimulation area (Experiment 1) and stimulation frequency (Experiment 2). Experiment 3 served as a control experiment, where we expected that under electrical brain stimulation, recovered SSVEPs would be similar in waveform shape to the baseline SSVEPs. While SSVEP amplitude might be modulated by TES through resonance, its waveform shape should be similar within participants, if the TES artifact is correctly mitigated (see Dowsett et al 2020b, figure 3). Electrical stimulation without visual stimulation cannot elicit an SSVEP and should therefore result in a significantly weaker and uncorrelated signal. Looking ahead, we were indeed able to successfully record 40 Hz SSVEPs with EEG during brain stimulation. Testing different sites and frequencies, we did not find evidence for interactions.

2. Materials and methods

The rationale of this study was to investigate A) if obtaining clean EEG data during gamma-band pulsed tDCS, a form of oscillatory TES, is feasible; B) if gamma TES can augment SSVEPs elicited by gamma VS; and C) if different VS frequencies and TES sites affect the outcome. We hypothesised that to modulate visually evoked gamma activity, concurrent TES should be applied between occipital and central sites to target visual brain areas, and the frequency of both stimulation techniques should be closely matched (Ruhnau et al 2016, Dowsett et al 2020b). Experiments 1 and 2 aimed to test whether SSVEPs are enhanced by TES, depending on the factors site and frequency, respectively. After first processing the data from these experiments with an algorithm designed for alpha tACS (Dowsett et al 2020b), visual inspection revealed residual artifacts, so we followed up with Experiment 3 to improve and quantify artifact removal performance. Experiment 3 was then a control experiment, testing whether SSVEPs processed with our newly improved algorithm can be reliably dissociated from TES artifacts (not whether they are enhanced by TES,

as in Experiments 1 and 2). Upon confirming the effectiveness of the improved algorithm, we applied it to the data from all experiments. Those results are reported here. All data and code are openly available on OSF and GitHub, respectively.

2.1. Design

In all experiments, sessions began with TES and EEG setup and gradual habituation to TES and VS. Multiple blocks, each containing three (Experiments 1, 2) or four (Experiment 3) five-minute trials, were then recorded (figure 1(A)). During trials, participants were instructed to keep their eyes closed and centred and to remain still. They took short breaks between blocks with the VS mask lifted, room lights on, and eyes open. The TES frequency was always 39.9 Hz (see *Stimulation*).

In the first experiment, we aimed to rule out any effects of electrical currents on the retina or peripheral nerves as confounds (Kar and Krekelberg 2012, Thut et al 2017, Asamoah et al 2019) and investigate potential impacts of current direction (Balslev et al 2007). VS was applied at 40 Hz, and TES sites varied per block: we selected anodal O2 to cathodal Cz (O2-Cz+ or 'occipito-central') for the main condition, anodal Cz to cathodal O2 (Cz-O2+ or 'centro-occipital') as a reversed polarity condition, and anodal Cz to cathodal Fz (Cz-Fz+ or 'centro-frontal') as a site control (Herring et al 2019); see figure 1(B). In the second experiment, we tested for frequency specificity. TES was always anodal at O2 and cathodal at Cz, and VS frequency varied by block between 35, 40, and 45 Hz. The 40 Hz VS condition was equivalent to the occipito-central condition in Experiment 1; 35 and 45 Hz were frequency controls. Experiments 1 and 2 included three pseudorandomised blocks each: within every block, one trial of combined TES and VS was preceded and followed by a trial with only VS at the same VS frequency (figure 1(A)). VS-only trials that preceded combined VS and TES trials are referred to as 'baseline' trials (all PRE trials in figure 1(A)).

After applying the pipeline from (Dowsett et al 2020b) developed for the alpha band, the data from Experiments 1 and 2 revealed occasional residual TES artifacts appearing as square-shaped or spiked patterns, which could distort our results. Simulations revealed that this could be particularly problematic for the interpretation of Experiment 2, as residual artifacts in consecutive data segments time-locked to VS would be more likely to average out if VS and TES frequencies do not match (figure S1). This prompted us to run another experiment to systematically optimise and objectively quantify the artifact removal pipeline's performance. Experiment 3 comprised two pseudorandomised blocks (figure 1(A)): The experimental block started with a baseline trial of only 40 Hz VS, followed by the same three TES conditions as in Experiment 1 - occipito-central, centro-

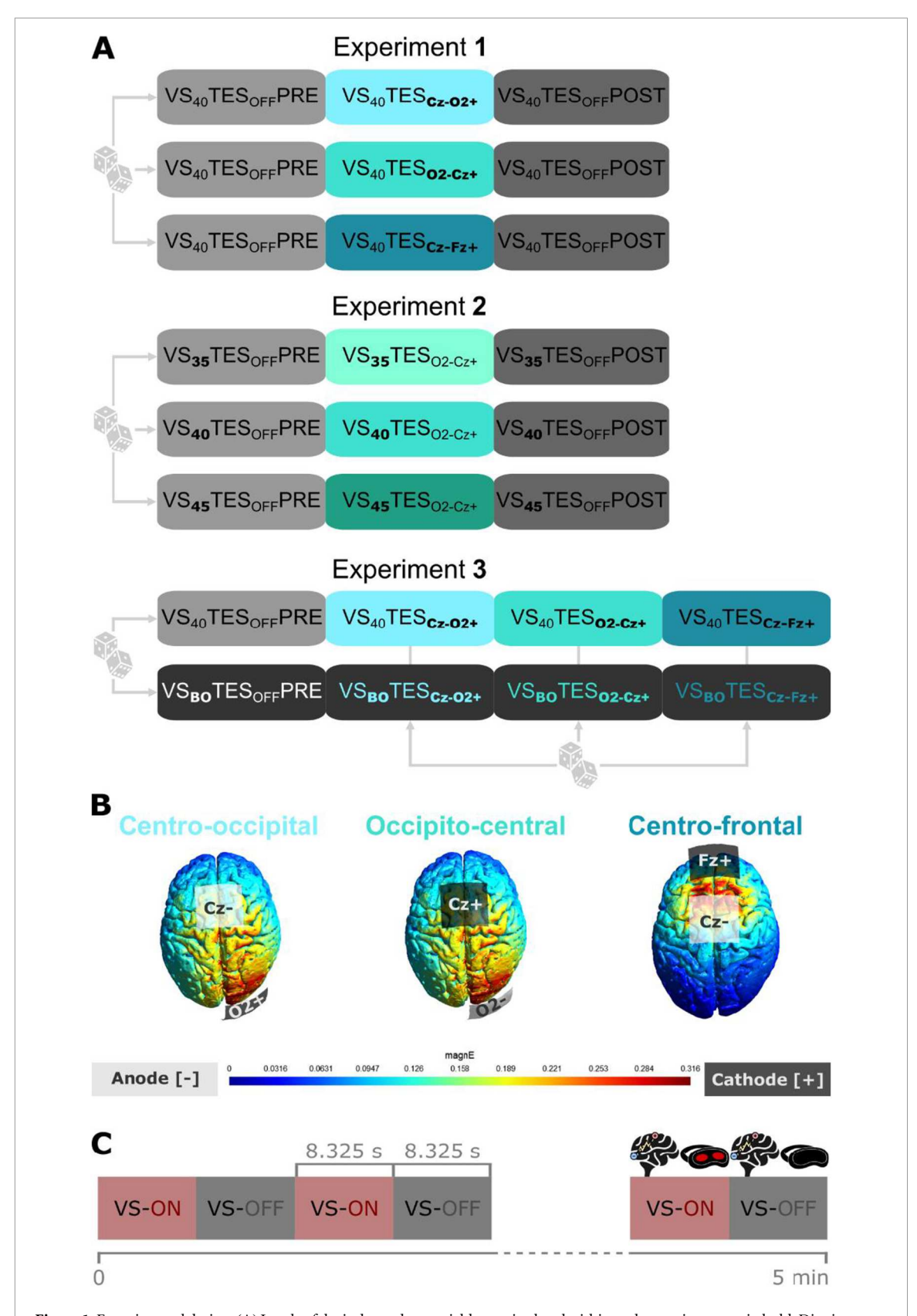


Figure 1. Experimental design. (A) Levels of the independent variable manipulated within each experiment are in bold. Dice icons represent pseudorandomisation. One box equals one 5-minute trial; one row of three or four trials marks one block. VS = Visual Stimulation at a frequency of 35 Hz, 40 Hz, or 45 Hz, indicated by subscripts. In VS_{BO} (BO for 'blackout'), the LEDs flickering at 40 Hz were covered with black tape. PRE = a baseline trial without TES, recorded *before* a trial with TES; POST = a trial without TES, recorded *after* a trial with TES. TES = Transcranial Electrical Stimulation at 39.9 Hz, either Cz anodal and O2 cathodal (Cz-O2+), O2 anodal and Cz cathodal (O2-Cz+), Cz anodal and Fz cathodal (Cz-Fz+) or no electrical stimulation (OFF), indicated by subscripts. (B) Simulation of current flows for the three TES montages. The centro-occipital montage is equivalent to the occipitocentral one with reversed polarity; they are equivalent here because the models display the absolute amplitude of the electric field. magnE = absolute magnitude of the electric field in V/m. (C) Structure of all trials where TES was applied. TES was always on throughout the full 5 min of a trial. VS (blackout or visible) alternated between on for 8.325 s and off for 8.325 s.

Table 1. Sample demographics.

Experiment	Sample size	Age mean (years)	Age range (years)	Sex ^a	Handedness
1	25	23.08	18–28	$18\mathrm{F}/7\mathrm{M}$	21 RH/3 LH/1 AD
2	25	23.76	18-28	$17\mathrm{F}/8\mathrm{M}$	21 RH/3 LH/1 AD
3	25	26.4	18–30	$15\mathrm{F}/10\mathrm{M}$	$22\mathrm{RH}/3\mathrm{LH}$

F = female; M = male; RH = right-handed; LH = left-handed; AD = ambidextrous.

occipital, and centro-frontal - with simultaneous 40 Hz VS. The defining feature of Experiment 3 was the 'blackout' control block, where the VS device was on at 40 Hz, but the LEDs were covered with black tape. This precluded any visual stimulation effects while keeping control conditions electrically equivalent. The control block started with a resting state trial, with blackout VS and no TES. Three trials followed, matching the TES configurations of the experimental block but with blackout VS (figure 1(A)). Any rhythmic signals captured in these trials could only result from residual TES artifacts, not SSVEPs, which cannot be evoked if VS light does not reach the retina. The order of TES trials was also pseudorandomised and kept constant in both blocks within participants.

2.2. Sample

With approval by the LMU Munich Psychology ethical committee [19-688, October 2023] and written informed consent obtained from all participants, we recruited 25 healthy adult volunteers per experiment. All procedures complied with the Declaration of Helsinki, relevant laws, institutional guidelines, and participants' privacy rights. Ten volunteers took part in Experiments 1 and 2, three volunteers took part in Experiments 2 and 3, and eleven participated in all three Experiments. Their sessions were at least one month apart. The exclusion criteria were a history of seizures or epilepsy (also for first-degree relatives), any psychiatric or neurological condition, and colour blindness assessed with an Ishihara test (Ekhlasi et al 2021, Clark 1924). The demographic information is summarised in table 1.

2.3. Stimulation

Transcranial Electrical Stimulation (TES) was administered using the neuroConn DC-Stimulator Plus (neuroCare Group GmbH, Munich, Germany). We used 5 × 5 cm square rubber electrodes with Ten20 conductive paste (Weaver and Company, Colorado, USA). Impedances were kept below 10 kOhm. The O2, Cz, and Fz positions were defined according to the 10–20 system, based on a previous study (Dowsett *et al* 2020b). Current flows simulated for a tDCS pulse using one author's brain scans and SimNIBS software (Saturnino *et al* 2019) are shown in figure 1(B). The stimulation waveform was delivered to the stimulator with a digital-to-analogue converter using the 'remote input' function. The pulsed Transcranial Direct

Current Stimulation oscillated between 0 and 0.8 mA in a square-wave pattern with a duty cycle of 50%. A squared pattern is more likely to modulate neuronal responses (Fröhlich and McCormick 2010, Sherfey et al 2018) and facilitates artifact removal (Dowsett et al 2020b); direct current allows for a test of polarity effects, as opposed to alternating current. The current strength of 0.8 mA was chosen as a compromise between participant comfort, artifact size, and effectiveness. The TES frequency of 39.9 Hz used in all experimental conditions, just below the VS frequency of interest at 40 Hz, allowed for phase shifts between TES and VS, such that the VS and TES gradually drifted out of phase. We stimulated across all phases as the optimal stimulation phase is unknown; it may differ across participants, and multiple phases may elicit an effect. Cycling through all phases allows for measuring the average effect (Dowsett et al 2020b). Moreover, any TES artifacts remaining after data processing would be distributed across phase bins, averaging to zero given enough data. During TES trials, TES was administered continuously for five minutes.

Visual stimulation (VS) was delivered through a custom-made system powered by a microcontroller, with LEDs embedded in a mask blocking off any external light. We chose this setup for its highly precise timing and because it does not induce electrical artifacts, as previously validated (Hainke et al 2025). Participants' eyes were closed as in Hainke et al where VS was administered during sleep, laying the ground for a future application of the present multimodal protocol during sleep. Here, the eyes-closed protocol also helped to mitigate signal contamination by eye blinks and microsaccades—important physiological confounds sharing the gamma frequency range—and to stimulate for long times without the side effect of eye fatigue (Hipp and Siegel 2013, Schielke and Krekelberg 2022). 'Flickering' light was temporally modulated in a square-wave pattern at a duty cycle of 50%. Narrowband red light with a peak wavelength of 605 nm facilitated transmittance through closed eyelids (Bierman et al 2011); the target illuminance was 175 photopic lux at the eye, a value chosen based on pilot tests. In every five-minute trial, the temporally modulated light alternated between ON and OFF periods, each 8.325 s long (figure 1(C)). This duration ensured that for the primary frequency of interest of 40 Hz, the TES and VS cycles drifted apart long

^a All participants indicated that their gender matched their sex assigned at birth.

enough to cover all relative phases in one ON-period. Phase distributions were equally unbiased for 35 Hz and 45 Hz VS (Figure S2). ON-periods originally containing both SSVEPs and TES artifacts were processed and then used for statistical analyses. OFF-periods containing only TES artifacts and no neural signal of interest were used for artifact removal. This applies equally to blackout trials in Experiment 3, where the LEDs were covered with black tape.

2.4. EEG acquisition and processing

EEG data were recorded with a BrainAmp system (Brain Products GmbH, Gilching, Germany) at a 5 kHz sampling rate and impedances below 10 kOhm. The ground was placed on the left earlobe, the reference on the right earlobe, and the active electrode at the midpoint between the two main TES electrodes at O2 and Cz (near P2), where the electrical artifact would be smallest. Due to individual differences in head morphology, when needed, the active electrode was adjusted slightly until the raw data showed the characteristic TES square shape and did not clip. A DC correction was applied before every block to prevent signal saturation by the TES electric charge. Data were divided into short segments time-locked to the flicker, with a length depending on VS frequency of 22.2 ms (45 Hz), 25 ms (40 Hz), or 28.8 ms (35 Hz). Data were not filtered to prevent distorting the shape of the TES artifact.

To clean EEG data segments of TES artifacts, we refined the Adaptive Template Subtraction method by (Dowsett et al 2020b). We refer to the updated algorithm described below as ATS. The pipeline's feature and parameters were optimised solely based on data from VS_{BO}TES_{O2-Cz+}, the control condition from Experiment 3 directly matching the main experimental condition included in all three experiments, VS₄₀TES_{O2-Cz+}. In VS_{BO}TES_{O2-Cz+}, no VS was visible, so no neural signal of interest (i.e., SSVEP) could be evoked; also, segments were time-locked to the (unseen, blacked-out) 40 Hz VS and not to TES at 39.9 Hz. Thus, if the pipeline correctly removes TES artifacts, the segment average should be a relatively flat line. Any slight fluctuations should only reflect natural EEG noise, not a periodic 39.9 Hz signal. Simulations revealed how an average signal resembling a 40 Hz SSVEP could appear in control data if the artifact removal were to perform suboptimally in a larger number of consecutive segments (Figure S1). Therefore, modifications to the pipeline were deemed successful if they further minimised median peak-to-peak amplitudes of participant-level segment averages in the condition VS_{BO}TES_{O2-Cz+}. Only after the pipeline optimisation was concluded did we apply it universally to all data across all conditions and experiments, to prevent any bias in our statistical analyses.

Each segment-to-clean in VS-ON periods of TES trials underwent the processing pipeline visualised in figure 2(A) and described as follows. First, the steepest

points of the segment-to-clean were defined as the data points where its absolute first differential exceeded 10% of the segment's total amplitude ('steepest points'). The first differential of a time series quantifies the steepness of transitions between neighbouring time points. For a 25 ms segment, for example, this typically resulted in one subset of data points for the TES square-wave rise and one subset for the TES square-wave fall. These steep point subsets were each extended by two data points before and four data points after, to capture the full extent of the artifact ('artifact points'). Then, segments potentially suitable for a template were selected from two VS-OFF periods - the one before and the one after the current VS-ON period (except if the segment-to-clean was in a trial's first VS-ON period, then only the directly following VS-OFF period was available). VS-OFF data were digitally segmented with a sliding window matching the length of the segment-to-clean and moving forward one data point at a time. The peak-to-peak amplitude was computed for each VS-OFF segment minus the segment-to-clean; if this value was below 10% of the segment-to-clean's amplitude, the VS-OFF segment was pre-selected as a potential candidate for the template. Each pre-selected VS-OFF segment was assigned a score computed by subtracting the segment-to-clean from the VS-OFF segment, taking the first differential of this difference, and calculating the sum across the 'artifact points'. The best combination of VS-OFF segments for a template was defined as the pair for which the absolute average score was the lowest. Because the first differential quantifies steepness between neighbouring data points, a low absolute score derived from the points most affected by the rising or falling artifact indicates a good match between segment-to-clean and template. The two best VS-OFF segments of approximately 300 were averaged into a template; then, the template was scaled to best match the amplitude of the segment-to-clean. The template was progressively scaled larger or smaller as long as this reduced the maximum of the absolute first differential at the 'artifact points' of the segment-to-clean minus the scaled template. Lastly, the final template was baseline-corrected and subtracted from the baseline-corrected segment-to-clean.

The next step of the pipeline, depicted in figure 2(B), dealt with any artifacts that resisted the above-mentioned procedure. They could either appear as patterns resembling the TES pulse square shape or as sharp spikes at the TES rise or fall points, in case the template's shape or phase did not match the segment-to-clean well enough. This could result from a temporary increase in noise in the data, especially from a head movement. We first targeted the spike artifacts through linear interpolation: each segment after template subtraction was assigned a score, defined as the sum of its absolute first differential at the 'steepest points'. If this score exceeded the systematically calibrated threshold of $16\,\mu\text{V}$ (figure S3), the

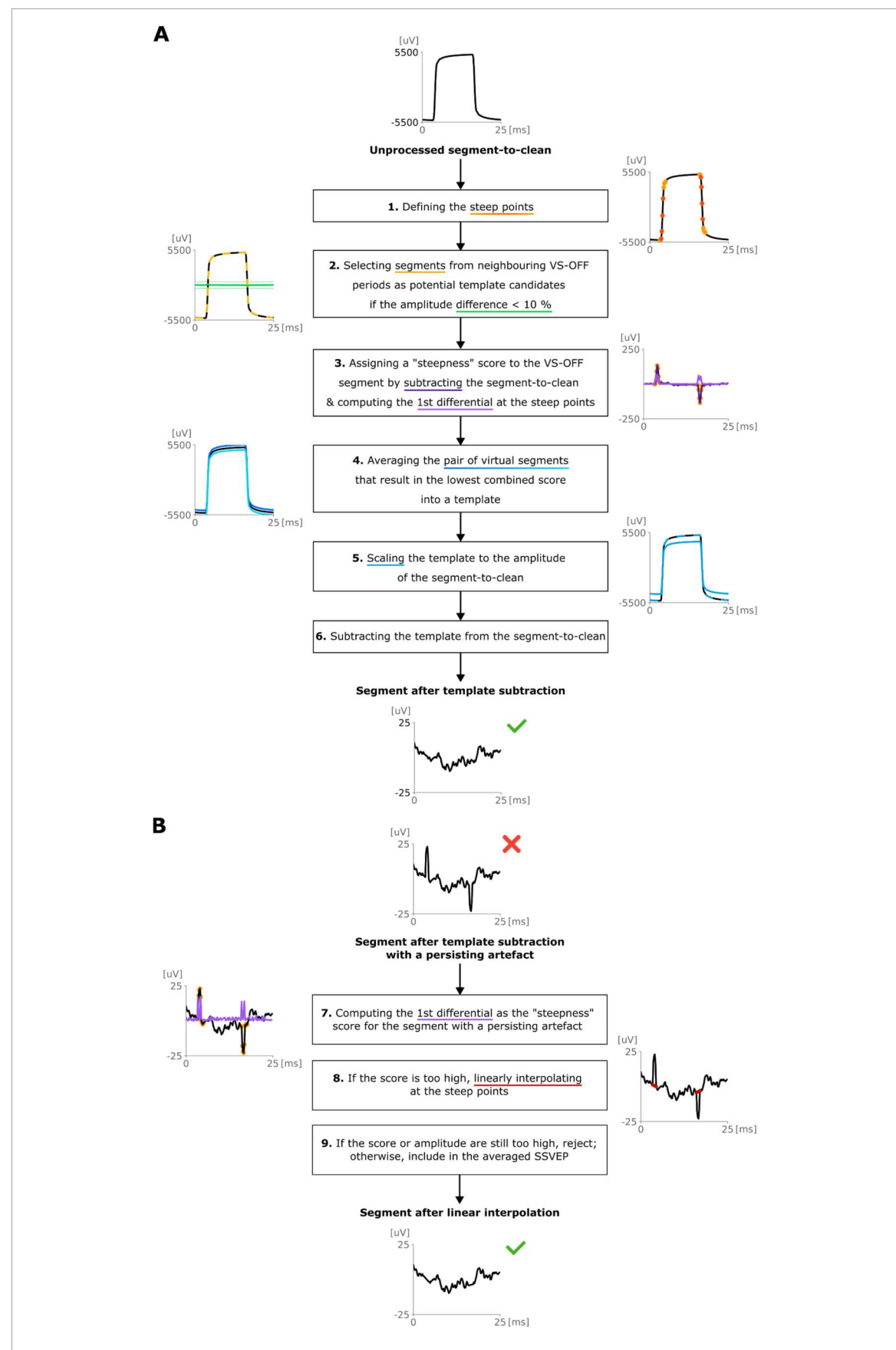


Figure 2. ATS pipeline for TES artifact removal. (A) Artifact removal process for all segments in VS-ON periods, recorded during concurrent TES and time-locked to the flicker. Segment lengths of 25 ms depicted here correspond to 40 Hz VS, but the same applies to 22.2 ms or 28.8 ms segments (35 Hz or 45 Hz VS). An example segment of data from Experiment 1, condition $VS_{40}TES_{O2-Cz+}$ is shown - with TES artifact before processing (first subplot) and after processing (last subplot). (B) Additional processing steps to mitigate artifacts surviving the processing pipeline depicted in A.

'steepest points' subsets were each replaced with a straight line. If the segment's score, recalculated after linear interpolation, still exceeded the threshold, a square-shaped artifact was likely present, so the segment was rejected.

Apart from these scores, three other criteria were defined for segment rejection post-processing: Segments in the first four seconds of each TES trial were discarded by default because muscular activity tended to be slightly higher at trial start, increasing the likelihood of residual artifacts. Second, segments for which fewer than two suitable template segments were found were removed. Lastly, as is common in standard EEG processing, segments with a peak-topeak amplitude larger than 90 µV (likely to contain muscular artifacts) were excluded. This last step also applied to segments from TESOFF conditions, which (free from TES artifacts by design) did not require any further processing. SSVEPs were finally computed by averaging all included segments by condition and participant, akin to a time-domain Event-Related Potential (figures S4–S9). The peak-to-peak amplitude of the time-domain segment average represents the SSVEP's magnitude.

To summarise the development of the ATS algorithm in this paper in the context of previous work: we started by using the previous algorithm that we had developed for a different dataset using saw-tooth tACS in the alpha-band (Dowsett *et al* 2020b). However here, by comparison, we used square-wave pulsed tDCS in the gamma band, and we found we needed to adapt the pipeline in three ways: 1) including a pair of segments for the base artifact template; 2) template scaling; 3) linear interpolation and rejection of processed segments. Figure 2 shows the complete ATS pipeline applied here to all three experiments.

2.5. Statistical analysis

In Experiments 1 and 2, we hypothesised an increase in SSVEP amplitudes only by frequency-matched TES applied between occipital and central sites. Aftereffects were also tested for in these conditions. In Experiment 3, we tested for residual TES artifacts by comparing TES-only conditions to resting-state data. Moreover, we hypothesised that SSVEPs evoked by 40 Hz VS could be recovered during frequencymatched TES at all sites, evidenced by A) larger amplitudes than the averaged signal from corresponding TES-only control data without VS and B) higher waveform correlations with baseline SSVEPs from VS-only data than with averaged signals from TES-only data. With a significance criterion of $\alpha = 0.05$ and Cohen's d as effect size, directed hypotheses were tested through one-tailed permutation tests, and two-tailed permutation tests were run for expected null effects. Pearson correlation coefficients to assess SSVEP waveform similarity between two conditions were also subjected to permutation

tests. Participants were excluded from a test if less than half of the data was available for any condition in that test. Bonferroni-corrected p-values to account for multiple comparisons are reported in the Supplementary Materials (tables S1–3).

3. Results

The results of Experiment 1 are detailed in table 2. Contrary to expectations, centro-occipital frequency-matched TES did not modulate SSVEP amplitudes during stimulation (H1.1), and occipito-central frequency-matched TES slightly decreased them (H1.3), though this effect does not survive Bonferroni correction (p = .1; table S1). Neither of these TES configurations induced after-effects on SSVEPs (H1.2, H1.4). As expected, centro-frontal frequency-matched TES did not increase SSVEP amplitudes during or after stimulation (H1.5, H1.6).

The results of Experiment 2 are listed in table 3. Frequency-matched occipito-central TES again did not increase SSVEP amplitudes during (H2.3) and after (H2.4) stimulation. As expected, when VS frequency was lower (35 Hz) or higher (45 Hz) than TES frequency, occipito-central TES did not modulate SSVEP amplitudes during stimulation (H2.1, H2.5). SSVEP amplitudes after TES were unaltered in the 35 Hz VS condition (H2.2) and decreased in the 45 Hz condition (H2.6).

Table 4 summarises the results of Experiment 3. While TES artifacts are unlikely to be eliminated entirely (Kasten and Herrmann 2019; H3.1, H3.3, H3.5), here they have been successfully minimised to a level smaller than the neural signal of interest. The averaged signal from conditions with both visual and electrical stimulation, baseline-corrected by data unaffected by any stimulation, had a larger amplitude than in conditions with electrical stimulation alone, equally baseline-corrected. This is true for occipitocentral and centro-occipital TES (H3.2, H3.4); the test for centro-frontal TES did not reach significance (H3.6). It follows that apart from centro-frontal TES conditions, recording neuronal responses evoked by VS with EEG was possible despite the ongoing brain stimulation with occipital and central TES (figure 3).

SSVEP waveform correlations further supported this finding. Note that while TES-only trials may contain residual artifacts but no visually evoked neural signal, the opposite is true for VS-only trials. Our data show that the averaged signal from the conditions combining VS and TES was more highly correlated with the signal acquired during VS-only than with the signal acquired during TES-only (H3.7, H3.8). Figure 4 displays the participant-level SSVEPs. Regardless of whether TES was applied simultaneously or not, recovered waveforms tended to be noticeably similar within participants, semi-sinusoidal, and consistent with a VS frequency of 40 Hz in

 Table 2. Results of Experiment 1.

	Variable 1	Test	Variable 2	N	Mean (SD) 1	Mean (SD) 2	Mean difference [Confidence Interval]	P-value	Cohen's d
H1.1	VS ₄₀ TES _{OFF} PRE	<	VS ₄₀ TES _{Cz-O2+}	25	1.44 (0.8)	1.47 (0.75)	0.04[-0.11;0.18]	0.31	0.03
H1.2	$VS_{40}TES_{OFF}PRE$	<	$VS_{40}TES_{OFF}POST$	25	1.44(0.8)	1.39 (0.84)	-0.05[-0.15;0.05]	0.18	-0.04
H1.3	$VS_{40}TES_{OFF}PRE$	<	$VS_{40}TES_{O2-Cz+}$	25	1.52 (0.83)	1.36 (0.71)	-0.16[-0.32;0.01]	0.03	-0.14
H1.4	$VS_{40}TES_{OFF}PRE$	<	$VS_{40}TES_{OFF}POST$	25	1.52 (0.83)	1.48 (0.85)	-0.03[-0.2;0.13]	0.32	-0.03
H1.5	$VS_{40}TES_{OFF}PRE$	=/=	$VS_{40}TES_{Cz-Fz+}$	25	1.46 (0.89)	1.17 (0.6)	-0.29[-0.58;-0.01]	0.05	-0.27
H1.6	$VS_{40}TES_{OFF}PRE$	=/=	$VS_{40}TES_{OFF}POST$	25	1.46 (0.89)	1.39 (0.82)	-0.08[-0.22;0.07]	0.27	-0.06

Means, standard deviations (SD), and confidence intervals in microvolts. The symbol '<' indicates the direction of one-tailed tests; '=/=' represents two-tailed tests for expected null effects. PRE and POST refer to the VS-only trials before and after the TES condition within a given block, respectively—i.e., Cz-O2+ in H1.1 and H1.2, O2-Cz+ in H1.3 and H1.4, and Cz-Fz+ in H1.5 and H1.6.

Table 3. Results of Experiment 2.

	Variable 1	Test	Variable 2	N	Mean (SD) 1	Mean (SD) 2	Mean difference [Confidence Interval]	P-value	Cohen's d
H2.1	VS ₃₅ TES _{OFF} PRE	<	VS ₃₅ TES _{O2-Cz+}	24	1.64 (0.78)	1.51 (0.74)	-0.12 [-0.29; 0.05]	0.16	-0.11
H2.2	$VS_{35}TES_{OFF}PRE$	<	VS ₃₅ TES _{OFF} POST	24	1.64 (0.78)	1.57 (0.84)	-0.06[-0.34;0.21]	0.61	-0.05
H2.3	$VS_{40}TES_{OFF}PRE$	<	$VS_{40}TES_{O2-Cz+}$	23	1.15 (0.51)	1.16 (0.47)	0.0[-0.14;0.15]	0.47	0.01
H2.4	$VS_{40}TES_{OFF}PRE$	<	$VS_{40}TES_{OFF}POST$	23	1.15 (0.51)	1.15 (0.52)	-0.01[-0.12;0.1]	0.42	-0.01
H2.5	$VS_{45}TES_{OFF}PRE$	=/=	$VS_{45}TES_{O2-Cz+}$	24	0.9 (0.34)	0.82 (0.29)	-0.08[-0.17;0.01]	0.07	-0.18
H2.6	$VS_{45}TES_{OFF}PRE$	=/=	${\rm VS_{45}TES_{OFF}POST}$	24	0.9 (0.34)	0.75 (0.3)	-0.15[-0.23;-0.07]	<.01	-0.32

Means, standard deviations (SD), and confidence intervals in microvolts. The symbol '<' indicates the direction of one-tailed tests; '=/=' represents two-tailed tests for expected null effects.

_

Table 4. Results of Experiment 3.

	Variable 1	Test	Variable 2	N	Mean (SD) 1	Mean (SD) 2	Mean difference [Confidence Interval]	P-value	Cohen's d
H3.1	VS _{BO} TES _{OFF} PRE	=/=	VS _{BO} TES _{Cz-O2+}	21	0.32 (0.07)	0.66 (0.21)	0.34 [0.24; 0.45]	<.01	1.56
H3.2	$VS_{BO}TES_{Cz-O2+} - VS_{BO}TES_{OFF}PRE$	<	$VS_{40}TES_{Cz-O2+} - VS_{BO}TES_{OFF}PRE$	21	0.34(0.23)	0.72 (0.42)	0.37 [0.18; 0.56]	<.01	0.78
H3.3	$VS_{BO}TES_{OFF}PRE$	=/=	$VS_{BO}TES_{O2-Cz+}$	20	0.31 (0.07)	0.67 (0.23)	0.35 [0.25; 0.45]	<.01	1.49
H3.4	$VS_{BO}TES_{O2-Cz+} - VS_{BO}TES_{OFF}PRE$	<	$VS_{40}TES_{O2-Cz+} - VS_{BO}TES_{OFF}PRE$	20	0.35 (0.21)	0.93 (0.51)	0.58 [0.33; 0.82]	<.01	1.04
H3.5	$VS_{BO}TES_{OFF}PRE$	=/=	$VS_{BO}TES_{Cz-Fz+}$	18	0.31 (0.06)	0.62(0.2)	0.3 [0.2; 0.41]	<.01	1.44
H3.6	$VS_{BO}TES_{Cz-Fz+}$ $-VS_{BO}TES_{OFF}PRE$	<	$VS_{40}TES_{Cz-Fz+} - VS_{BO}TES_{OFF}PRE$	18	0.3 (0.21)	0.41 (0.21)	0.11[-0.06;0.27]	0.09	0.36
H3.7	$VS_{40}TES_{O2-Cz+} X VS_{BO}TES_{O2-Cz+}$	<	$VS_{40}TES_{O2-Cz+} X VS_{40}TES_{OFF}PRE$	20	0.27(0.54)	0.7 (0.33)	0.44 [0.12; 0.76]	<.01	0.7
H3.8	$VS_{40}TES_{Cz\text{-}O2+}XVS_{BO}TES_{Cz\text{-}O2+}$	<	$VS_{40}TES_{Cz\text{-}O2+}XVS_{40}TES_{OFF}PRE$	21	-0.04(0.52)	0.76 (0.38)	0.8 [0.51; 1.09]	<.01	1.25

Means, standard deviations (SD), and confidence intervals in microvolts, except for H3.7 and H3.8 (unit-free correlation coefficients). The symbol '<' indicates the direction of one-tailed tests; '=/=' represents two-tailed tests for expected null effects; 'X' stands for Pearson correlations of SSVEP waveforms.

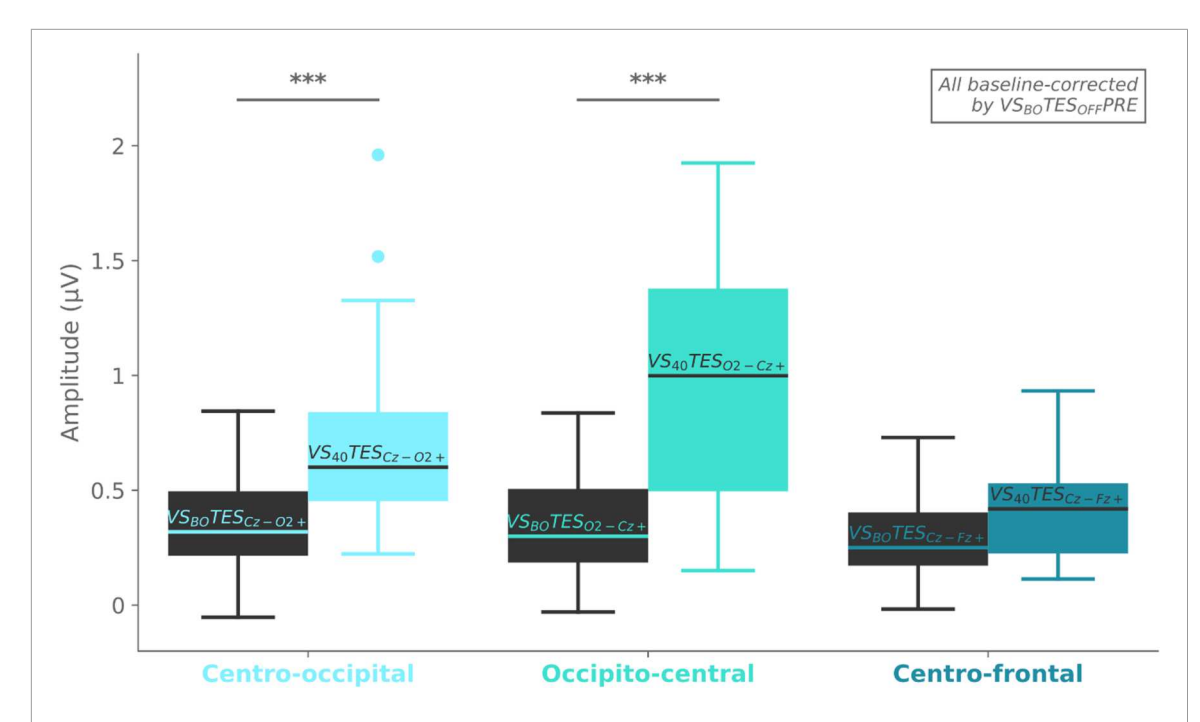


Figure 3. Visual responses (SSVEPs) successfully recovered with EEG during TES applied between central and occipital electrodes. Peak-to-peak amplitudes of averaged segments by condition in Experiment 3. Black boxplots represent conditions with blackout VS (VS_{BO}) and active TES; these signals may contain residual TES artifacts, but no visually evoked neuronal activity. Coloured boxplots represent the equivalent conditions with visible 40 Hz VS (VS₄₀); these signals should additionally contain visually evoked neuronal activity at 40 Hz. All were baseline-corrected by the resting-state condition with blackout VS and no TES (VS_{BO}TES_{OFF}PRE). Boxplot lines mark median values; boxes delimit the interquartile range; whiskers encompass data points within 1.5x of the interquartile range from box limits; *** = p < .001.

period. Group-level averages of SSVEP waveforms are not displayed, since averaging over participant-level SSVEPs of different phases and shapes would result in little signal (Dowsett *et al* 2020a). Instead, the significant group-level tests H3.7 and H3.8 support the generalisability of this finding.

The statistical results of Experiment 3 confirm that the ATS algorithm presented in this study effectively mitigates gamma TES artifacts, which was the aim of this experiment. It would be beyond the scope of the current study to systematically compare the current algorithm with previous approaches. Our focus here was to evaluate the current approach for artifact removal rather than to apply statistical analyses on clearly contaminated data, i.e., unprocessed data (figure 5(A)) or data processed with the previous algorithm designed for alpha tACS (figure 5(B)). Instead, figure 5(C) illustrates how data segments were appropriately cleaned with the present ATS algorithm, as confirmed statistically.

4. Discussion

In sum, we demonstrated that recording brain responses to 40 Hz visual flicker during frequency-matched TES is possible. Capturing EEG signals during TES remains a major challenge in neuromodulation, as TES artifacts vastly exceed neuronal signals especially in the gamma band, where a frequency overlap with physiological artifacts is problematic,

and when TES is frequency-matched to VS. Here, we demonstrate the efficacy of an improved Adaptive Template Subtraction method in successfully recovering 40 Hz SSVEPs during frequency-matched oscillatory TES. Although frequency-matched TES did not augment SSVEPs, our data strongly indicate genuine neuronal activity rather than electrical or physiological artifacts. These findings pave the way for fundamental and clinical research to combine rhythmic sensory and electrical gamma-band stimulation while concurrently verifying neuronal effects with EEG.

In Experiments 1 and 2, we tested whether oscillatory TES could enhance SSVEP amplitudes depending on TES sites and frequency overlap with VS. Our data did not support this hypothesis. The 0.8 mA TES current—chosen to balance participant comfort, artifact suppression, and efficacy—may have been too weak. It may have failed to influence the robust 40 Hz responses driven by widespread, dynamic visual processing - especially those elicited by square-wave flicker (Panitz et al 2023). This would be in line with a recent study showing the superiority of periodic sensory stimuli over concurrent TES in entraining behaviour (Cabral-Calderin and Henry 2025). The apparent decrease of 45 Hz SSVEP amplitudes after occipito-central TES in Experiment 2 may be coincidental, given ongoing debate over TES efficacy (Parkin et al 2015, Polanía et al 2018), the limitations of p-values for inferring effect importance (Rothman 2016, Wasserstein and Lazar 2020), the small effect

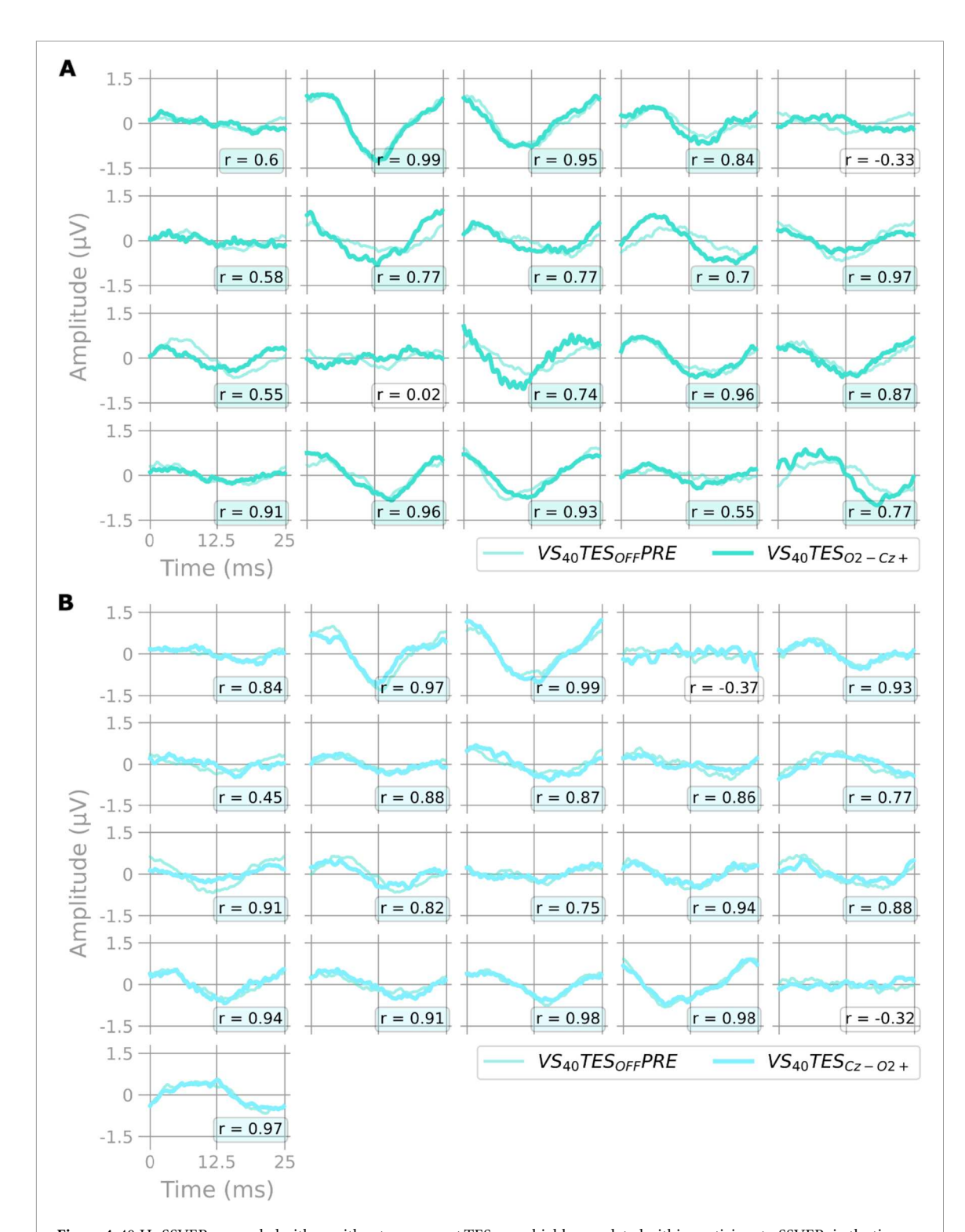


Figure 4. 40 Hz SSVEPs, recorded with or without concurrent TES, were highly correlated within participants. SSVEPs in the time domain at the participant level. Data were taken from Experiment 3 and processed as described in *EEG Acquisition & Processing*. Within-participant Pearson correlation coefficients of the two conditions' average waveforms are presented at the bottom right of every subplot and coloured if r > 0.4. (A) SSVEPs from the occipito-central condition. N = 20 after exclusion (see *Statistical Analysis*). VS₄₀TES_{OFF}PRE: 40 Hz Visual Stimulation and concurrent Transcranial Electrical Stimulation at 39.9 Hz, anodal at the occipital site O2 and cathodal at the central site Cz. (B) SSVEPs from the centro-occipital condition. N = 21 after exclusion (see *Statistical Analysis*). VS₄₀TES_{OFF}PRE: 40 Hz Visual Stimulation alone, the same as in A. VS₄₀TES_{Cz-O2+}: 40 Hz Visual Stimulation and concurrent Transcranial Electrical Stimulation at 39.9 Hz, anodal at the central site Cz and cathodal at the occipital site O2.

size (d = -0.32), and the lack of replication of after-effects across conditions. SSVEP variability may have stemmed from fatigue, differing sample characteristics, and varying condition orders.

One possibility is that TES at 39.9 Hz, drifting in and out of phase with 40 Hz VS, may have enhanced SSVEPs at some phases and suppressed them at others. We prioritised validating the data processing

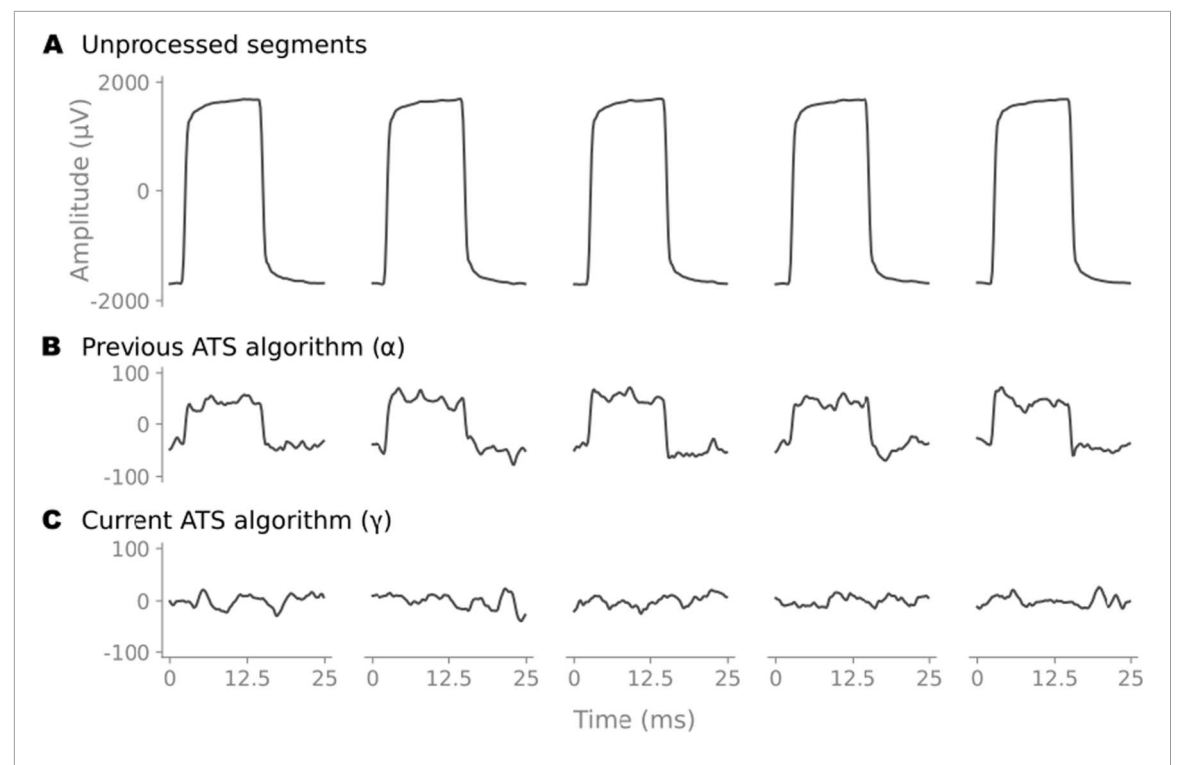


Figure 5. Only ATS adapted to gamma effectively mitigates gamma TES artifacts. Example 25 ms data segments from an individual participant, $VS_{BO}TES_{O2-Cz+}$ condition, baseline-corrected. (A) Raw segments without any processing. The squared TES shape dominates the signal at a high amplitude (note the higher *y*-axis limits). (B) The same segments processed with an ATS algorithm originally developed for alpha tACS (Dowsett *et al* 2020b). Residual square-shaped artifacts contaminate the EEG signal. (C) The segments processed with the ATS algorithm presented in this study. No residual artifact is visible.

pipeline in this study, reasoning that a uniform TES-VS phase distribution would aid interpretation, given the persistent challenge of artifact removal and the lack of consensus on an optimal stimulation phase. With artifact correction now validated, future work could systematically vary TES-VS phase to identify potential phase-dependent effects, which may also differ across individuals. Although red light through closed eyes may have reduced retinal input, this method can reliably elicit SSVEPs even in sleep and at lower illuminance (Hainke et al 2025). Higher TES intensities could be explored using anaesthetic gels to reduce skin sensation (Kerstens et al 2022). Lastly, other gamma TES protocols such as tACS or sawtooth-wave tDCS may also be worth investigating (Dowsett and Herrmann 2016, Dowsett et al 2020b).

Experiment 3 highlighted the need for robust control conditions where TES is active but sensory input is blocked - especially when comparing different stimulation frequencies, since residual artifacts may affect SSVEPs more strongly when TES and VS frequencies match (figure S1). We confirmed that signals during combined visual and electrical stimulation over occipital and central areas were stronger than during electrical stimulation alone (figure 3). Although complete artifact removal remains challenging (Kasten and Herrmann 2019), our pipeline reduced TES artifact amplitude by a factor of 220. For example, in the main control condition (occipitocentral TES with blackout VS), average segment

amplitudes dropped from $6356\,\mu V$ (raw) to $28.9\,\mu V$ (processed) - well within the typical $0.5{\text -}100\,\mu V$ range of resting-state EEG (figure 5; Teplan 2002). In the centro-frontal TES condition, artifacts were too large to prevent signal saturation in all trials - likely due to strong electric field differences between active and reference electrodes. Our setup thus performs well for EEG electrodes positioned between TES electrodes, but will require adaptation for electrodes located farther from the TES midline. Future studies could address this by testing alternative EEG electrodes, TES electrode sizes, or TES shapes.

To further demonstrate the successful recovery of 40 Hz SSVEPs during TES, we compared waveform shapes. SSVEPs recorded during centro-occipital and occipito-central TES closely resembled baseline SSVEPs without TES, as would be expected within subjects (Dowsett *et al* 2020b) and differed from TES-only signals, which may contain residual artifacts but no visual response. Across VS conditions, SSVEPs exhibited semi-sinusoidal waveforms and periodicity consistent with 40 Hz visual stimulation. The within-subject similarity was both visually apparent (figure 4) and statistically significant.

This analysis, providing evidence for genuine neuronal activity as opposed to square-shaped artifacts, is by definition only possible with time-domain SSVEP processing. Unlike the FFT, this method is assumption-free regarding waveforms (Cole and Voytek 2017). Further advantages over traditional

frequency-domain analyses include a more fine-grained artifact removal that can adapt to TES artifact variations (e.g., caused by impedance changes) at millisecond scale. Moreover, averaging thousands of brief (e.g., 25 ms) segments yields a high signal-to-noise ratio, as confounds like muscular or ocular activity which share the gamma band (Hipp and Siegel 2013), but are not phase-locked to VS, average out.

We refrained from applying an FFT to our processed data for comparison, since our pipeline rejects segments with residual TES or physiological artifacts. It would be ill-fitting to treat the remaining segments as a continuous time series, misrepresenting the temporal dynamics of unprocessed neuronal activity. Moreover, the pipeline applies baseline correction to segments: Not realigning them would add sharp transitions to the data that may introduce spurious artifacts in the FFT, and realigning them would add low-frequency drifts. This pipeline is intended for use in the EEG time domain, which we argue to be a valid way to represent less commonly studied features of SSVEPs (Dowsett *et al* 2020a, Dowsett *et al* 2020b).

While the ATS method presented here builds on (Dowsett et al 2020b), several key differences distinguish our approach (see figure 2 here versus figure 2 in Dowsett et al 2020a). First, we used pulsed tDCS rather than tACS, enabling polarity-specific analyses. Second, we applied the more common square-wave instead of sawtooth stimulation. Third, we administered TES at 0.8 mA (versus 2 mA), guaranteeing comfort required for future use during sleep (Hainke et al 2025) or in clinical populations. Most critically, we used gamma-band stimulation, which poses greater challenges for EEG than alpha-band stimulation (Hipp and Siegel 2013). These differences likely explain the distinct patterns of results in both studies and why the original algorithm, designed for sawtooth alpha tACS, performed suboptimally on our initial data (figure 5(B)). This motivated Experiment 3, which included electrically equivalent control conditions to guide data-driven improvements. The updated ATS algorithm uses a pair of segments to form the base artifact template, instead of just one; this is particularly useful when two template segments match the phase of the segment to clean, but each at a higher or lower artifact amplitude, respectively. We also introduced template scaling for a better template fit, as well as linear interpolation and rejection of processed segments to handle any persisting residual artifacts.

Note that our question in this project was whether recovering gamma SSVEPs during frequency-matched TES is feasible. A systematic comparison between the improved ATS algorithm described here and any other artifact removal methods, although beyond the scope of the current study, is an important topic for future work. Through systematic improvements of the ATS algorithm, we were here able to reduce the artifacts and recover gamma SSVEPs - as

confirmed by visual inspection (figure 5(C)) and statistical tests (figures 3–4). The novel contribution of this study is the successful combination of VS and TES in the artifact-prone and neurophysiologically distinct gamma band at 40 Hz, beyond previous applications for alpha <11 Hz.

To conclude, we demonstrated that 40 Hz Steady-State Visually Evoked Potentials can be reliably measured with EEG during frequency-matched Transcranial Electrical Stimulation using Adaptive Template Subtraction, providing evidence in favour of recovered neuronal activity distinct from electrical or physiological confounds. This enables new applications combining sensory and electrical brain stimulation, both widely used to modulate human gamma activity (Thut et al 2011, Hanslmayr et al 2019, Koch et al 2024, Wang et al 2024). Future studies can systematically test how frequency-matched TES might modulate sensory-evoked potentials under various conditions, such as individual peak gamma frequencies (Mockevičius et al 2023), brain-computerinterfaces (Müller et al 2011, Bojorges-Valdez and Yanez-Suarez 2018), and other sensory domains (Jones et al 2020, Mosabbir et al 2022, Rufener et al 2023). Multimodal gamma stimulation might support the normalisation of gamma oscillations in various neurological and psychiatric conditions (Palmisano et al 2024) and neuroenhancement (Antal et al 2022, Camacho-Conde et al 2023, Violante and Okyere 2024). Importantly, as enhanced gamma activity likely underlies any cognitive effects, neuronal responses to stimulation should be quantified—this is now possible.

Acknowledgments

The authors would like to acknowledge Joshi Walzog and Oliver Holder from the Max-Planck Institute for Biological Cybernetics electronics workshop for developing the visual stimulation system, and all participants.

Data availability statement

The data that support the findings of this study are openly available at the following URL/DOI: https://osf.io/ut47g/. The code for data processing and analysis is openly available at the following URL/DOI: https://github.com/laura-hainke/HainkeEtAl_BPEX_2025.

Funding

This work was supported by the Deutsche Forschungsgemeinschaft (DFG) grants [DO 2460/1-1] to JD and [TA857/3-2] to PT, the Excellence Strategy of the Federal Government and the Länder through the NEUROTECH Innovation Network (IGSSE) to JP,

and the Max Planck Society to MS. The funders played no role regarding study design, collection, analysis and interpretation of data, writing of the report or the decision to submit the article for publication.

Declaration of interest

LH, PT, and JD report no conflicts of interest. JP is on the TSC of the Sinapps2 study and a board member of the following societies: DGPPN, DZPG, DZNE. MS is a member of the Board of Directors, Society of Light, Rhythms, and Circadian Health (SLRCH); Chair of Joint Technical Committee 20 (JTC20) of the International Commission on Illumination (CIE); Member of the Daylight Academy; Chair of Research Data Alliance Working Group Optical Radiation and Visual Experience Data, received honoraria from the ISGlobal, Research Foundation of the City University of New York and the Stadt Ebersberg, Museum Wald und Umwelt, Daimler und Benz Stiftung, and is named on European Patent Application EP23159999.4A ('System and method for corneal-plane physiologically-relevant light logging with an application to personalized light interventions related to health and well-being').

Author contributions

Laura Hainke © 0000-0002-8348-5554 Conceptualization (equal), Data curation (lead), Formal analysis (lead), Investigation (lead), Methodology (equal), Software (equal), Validation (lead), Visualization (lead), Writing – original draft (lead)

Manuel Spitschan © 0000-0002-8572-9268 Conceptualization (equal), Supervision (equal), Writing – review & editing (equal)

Josef Priller

Funding acquisition (equal), Supervision (equal), Writing – review & editing (equal)

Paul Taylor

Conceptualization (equal), Formal analysis (equal), Funding acquisition (equal), Methodology (equal), Project administration (equal), Resources (equal), Supervision (equal), Writing – review & editing (equal)

James Dowsett

Conceptualization (equal), Formal analysis (equal), Funding acquisition (equal), Investigation (equal), Methodology (equal), Project administration (equal), Resources (equal), Software (equal), Supervision (equal), Validation (equal), Writing – review & editing (equal)

References

- Antal A et al 2022 Non-invasive brain stimulation and neuroenhancement Clinical Neurophysiology Practice 7 146–65
- Asamoah B, Khatoun A and Mc Laughlin M 2019 tACS motor system effects can be caused by transcutaneous stimulation of peripheral nerves *Nat. Commun.* 10 266
- Balslev D, Braet W, McAllister C and Miall R C 2007 Interindividual variability in optimal current direction for transcranial magnetic stimulation of the motor cortex *J. Neurosci. Methods* 162 309–13
- Bayram A et al 2011 Simultaneous EEG/fMRI analysis of the resonance phenomena in steady-state visual evoked responses Clinical EEG and Neuroscience 42 98–106
- Bergmann T O, Karabanov A, Hartwigsen G, Thielscher A and Siebner H R 2016 Combining non-invasive transcranial brain stimulation with neuroimaging and electrophysiology: current approaches and future perspectives *NeuroImage* 140 4–19
- Bierman A, Figueiro M G and Rea M S 2011 Measuring and predicting eyelid spectral transmittance *J. Biomed. Opt.* **16** 067011
- Blanco-Duque C, Chan D, Kahn M C, Murdock M H and Tsai L-H 2023 Audiovisual gamma stimulation for the treatment of neurodegeneration *Journal of Internal Medicine* 295 146–70
- Bojorges-Valdez E and Yanez-Suarez O 2018 Association between EEG spectral power dynamics and event related potential amplitude on a P300 speller *Biomed. Phys. Eng. Express* 4
- Buzsáki G and Schomburg E W 2015 What does gammacoherence tell us about inter-regional neural communication? *Nat. Neurosci.* **18** 484–9
- Cabral-Calderin Y and Henry M J 2025 Sensory stimuli dominate over rhythmic electrical stimulation in modulating behavior PLoS Biol. 23 e3003180
- Camacho-Conde J A, del Rosario Gonzalez-Bermudez M,
 Carretero-Rey M and Khan Z U 2023 Therapeutic potential
 of brain stimulation techniques in the treatment of mental,
 psychiatric, and cognitive disorders *CNS Neurosci. Ther.* 29
 8–23
- Clark J H 1924 The Ishihara test for color blindness American Journal of Physiological Optics
- Cole S R and Voytek B 2017 Brain oscillations and the importance of waveform shape *Trends in Cognitive Sciences* 21 137–49
- Dowsett J, Dieterich M and Taylor P C J 2020a Mobile steady-state evoked potential recording: dissociable neural effects of real-world navigation and visual stimulation *J. Neurosci. Methods* 332 108540
- Dowsett J and Herrmann C S 2016 Transcranial alternating current stimulation with sawtooth waves: simultaneous stimulation and EEG recording Frontiers in Human Neuroscience 10 135
- Dowsett J, Herrmann C S, Dieterich M and Taylor P C J 2020b Shift in lateralization during illusory self-motion: EEG responses to visual flicker at 10 Hz and frequency-specific modulation by tACS *European Journal of Neuroscience* 51 1657–75
- Ekhlasi A, Ahmadi H, Molavi A, Saadat Nia M and Nasrabadi A M 2021 EEG signal analysis during Ishihara's test in subjects with normal vision and color vision deficiency *Biomed. Phys. Eng. Express* 7 025008
- Fröhlich F 2014 Endogenous and exogenous electric fields as modifiers of brain activity: rational design of noninvasive brain stimulation with transcranial alternating current stimulation *Dialogues Clin. Neurosci.* 16 93–102
- Fröhlich F and McCormick D A 2010 Endogenous electric fields may guide neocortical network activity *Neuron* 67 129–43
- Groppa S, Bergmann T O, Siems C, Mölle M, Marshall L and Siebner H R 2010 Slow-oscillatory transcranial direct current stimulation can induce bidirectional shifts in motor cortical excitability in awake humans *Neuroscience* 166 1219–25
- Guan A, Wang S, Huang A, Qiu C, Li Y, Li X, Wang J, Wang Q and Deng B 2022 The role of gamma oscillations in central nervous system diseases: mechanism and treatment *Frontiers*

- in Cellular Neuroscience 16 962957 (https://frontiersin.org/articles/10.3389/fncel.2022.962957)
- Güntekin B, Erdal F, Bölükbaş B, Hanoğlu L, Yener G and Duygun R 2022 Alterations of resting-state gamma frequency characteristics in aging and Alzheimer's disease Cognitive Neurodynamics 17 829–44
- Hainke L, Dowsett J, Spitschan M and Priller J 2025 40 Hz visual stimulation during sleep evokes neuronal gamma activity in NREM and REM stages SLEEP 48 zsae299
- Hanslmayr S, Axmacher N and Inman C S 2019 Modulating human memory via entrainment of brain oscillations *Trends in Neurosciences* 42 485–99
- Haslacher D, Nasr K, Robinson S E, Braun C and Soekadar S R 2021 Stimulation artifact source separation (SASS) for assessing electric brain oscillations during transcranial alternating current stimulation (tACS) NeuroImage 228 117571
- Herring J D, Esterer S, Marshall T R, Jensen O and Bergmann T O 2019 Low-frequency alternating current stimulation rhythmically suppresses gamma-band oscillations and impairs perceptual performance *NeuroImage* 184 440–9
- Herrmann C S 2001 Human EEG responses to 1–100 Hz flicker: resonance phenomena in visual cortex and their potential correlation to cognitive phenomena *Experimental Brain Research* 137 346–53
- Herrmann C S, Fründ I and Lenz D 2010 Human gamma-band activity: a review on cognitive and behavioral correlates and network models *Neuroscience & Biobehavioral Reviews* 34 981–92
- Herrmann C S, Rach S, Neuling T and Strüber D 2013 Transcranial alternating current stimulation: a review of the underlying mechanisms and modulation of cognitive processes *Frontiers in Human Neuroscience* 7 279 (https://frontiersin.org/articles/10.3389/fnhum.2013.00279)
- Hindriks R and van Putten M J A M 2013 Thalamo-cortical mechanisms underlying changes in amplitude and frequency of human alpha oscillations *NeuroImage* 70 150–63
- Hipp J and Siegel M 2013 Dissociating neuronal gamma-band activity from cranial and ocular muscle activity in EEG Frontiers in Human Neuroscience 7 338 (https://frontiersin.org/articles/10.3389/fnhum.2013.00338)
- Ichim A M, Barzan H, Moca V V, Nagy-Dabacan A, Ciuparu A, Hapca A, Vervaeke K and Muresan R C 2024 The gamma rhythm as a guardian of brain health *eLife* 13 e100238
- Jones K T, Johnson E L, Tauxe Z S and Rojas D C 2020 Modulation of auditory gamma-band responses using transcranial electrical stimulation *Journal of Neurophysiology* 123 2504–14
- Jonmohamadi Y and Muthukumaraswamy S D 2018 Multi-band component analysis for EEG artifact removal and source reconstruction with application to gamma-band activity Biomed. Phys. Eng. Express 4 035007
- Kar K and Krekelberg B 2012 Transcranial electrical stimulation over visual cortex evokes phosphenes with a retinal origin Journal of Neurophysiology 108 2173–8
- Kasten F H and Herrmann C S 2019 Recovering brain dynamics during concurrent tACS-M/EEG: an overview of analysis approaches and their methodological and interpretational pitfalls *Brain Topography* 32 1013–9
- Kerstens S, Orban de Xivry J-J and Mc Laughlin M 2022 A novel tDCS control condition using optimized anesthetic gel to block peripheral nerve input Frontiers Neurol. 13 1049409
- Kim D-W, Kim E, Lee C and Im C-H 2019 Can anodal transcranial direct current stimulation increase steady-state visual evoked potential responses? *Journal of Korean Medical Science* 34 e285
- Koch G, Altomare D, Benussi A, Bréchet L, Casula E P, Dodich A, Pievani M, Santarnecchi E and Frisoni G B 2024 The emerging field of non-invasive brain stimulation in Alzheimer's disease *Brain* 147 4003–16
- Li Z, Zhang R, Li W, Li M, Chen X and Cui H 2024 Enhancement of hybrid BCI system performance based on motor imagery and SSVEP by transcranial alternating current stimulation *IEEE Trans. Neural Syst. Rehabil. Eng.* 32 3222–30

- Liu B, Chen X, Yang C, Wu J and Gao X 2017 Effects of transcranial direct current stimulation on steady-state visual evoked potentials 39th Annual Int. Conf. of the IEEE Engineering in Medicine and Biology Society (EMBC) 2126–9
- Liu B, Yan X, Chen X, Wang Y and Gao X 2021 tACS facilitates flickering driving by boosting steady-state visual evoked potentials *J. Neural Eng.* 18 066042
- Mockevičius A, Šveistytė K and Griškova-Bulanova I 2023 Individual/peak gamma frequency: what do we know? *Brain Sciences* 13 792
- Mosabbir A A, Braun Janzen T, Al Shirawi M, Rotzinger S, Kennedy S H, Farzan F, Meltzer J and Bartel L 2022 Investigating the effects of auditory and vibrotactile rhythmic sensory stimulation on depression: an EEG pilot study *Cureus* 14 e22557
- Müller S M T, Diez P F, Bastos-Filho T F, Sarcinelli-Filho M, Mut V and Laciar E 2011 SSVEP-BCI implementation for 37–40 Hz frequency range *Annual Int. Conf. of the IEEE* Engineering in Medicine and Biology Society 6352–5 (10. 1109/IEMBS.2011.6091568)
- Nissim N R, Pham D V H, Poddar T, Blutt E and Hamilton R H 2023 The impact of gamma transcranial alternating current stimulation (tACS) on cognitive and memory processes in patients with mild cognitive impairment or Alzheimer's disease: a literature review *Brain Stimul*. 16748–55
- Noury N, Hipp J F and Siegel M 2016 Physiological processes nonlinearly affect electrophysiological recordings during transcranial electric stimulation *NeuroImage* 140 99–109
- Palmisano A, Pandit S, Smeralda C L, Demchenko I, Rossi S, Battelli L, Rivolta D, Bhat V and Santarnecchi E 2024 The pathophysiological underpinnings of gamma-band alterations in psychiatric disorders *Life* 14 578
- Panitz C, Gundlach C, Boylan M R, Keil A and Müller M M 2023 Higher amplitudes in steady-state visual evoked potentials driven by square-wave versus sine-wave contrast modulation —a dual-laboratory study *Psychophysiology* **60** e14287
- Parkin B L, Ekhtiari H and Walsh V F 2015 Non-invasive human brain stimulation in cognitive neuroscience: a primer Neuron 87 932–45
- Polanía R, Nitsche M A and Ruff C C 2018 Studying and modifying brain function with non-invasive brain stimulation *Nat.* Neurosci. 21 174–87
- Rothman K J 2016 Disengaging from statistical significance European Journal of Epidemiology 31 443—4
- Rufener K S, Zaehle T and Krauel K 2023 Combined multi-session transcranial alternating current stimulation (tACS) and language skills training improves individual gamma band activity and literacy skills in developmental dyslexia Developmental Cognitive Neuroscience 64 101317
- Ruhnau P, Keitel C, Lithari C, Weisz N and Neuling T 2016 Flickerdriven responses in visual cortex change during matchedfrequency transcranial alternating current stimulation Frontiers in Human Neuroscience 10 184 (https://frontiersin. org/articles/10.3389/fnhum.2016.00184)
- Saturnino G B, Puonti O, Nielsen J D, Antonenko D,
 Madsen K H and Thielscher A 2019 SimNIBS 2.1: a
 comprehensive pipeline for individualized electric field
 modelling for transcranial brain stimulation *Brain and Human Body Modeling: Computational Human Modeling at EMBC 2018* ed S Makarov, M Horner and G Noetscher
 (Springer International Publishing) 3–25 (10.1007/978-3030-21293-3_1)
- Schielke A and Krekelberg B 2022 Steady state visual evoked potentials in schizophrenia: a review *Frontiers in Neuroscience* 16 988077
- Sherfey J S, Ardid S, Hass J, Hasselmo M E and Kopell N J 2018 Flexible resonance in prefrontal networks with strong feedback inhibition *PLoS Comput. Biol.* 14 e1006357
- Shu I-W, Lin Y, Granholm E L and Singh F 2024 A focused review of gamma neuromodulation as a therapeutic target in Alzheimer's spectrum disorders *Journal of Psychiatry and Brain Science* 9 e240001

- Somer E, Allen J, Brooks J L, Buttrill V and Javadi A-H 2020 Theta phase-dependent modulation of perception by concurrent transcranial alternating current stimulation and periodic visual stimulation *Journal of Cognitive Neuroscience* 32 1142–52
- Strüber D and Herrmann C S 2020 Modulation of gamma oscillations as a possible therapeutic tool for neuropsychiatric diseases: a review and perspective *International Journal of Psychophysiology* **152** 15–25
- Teplan M 2002 Fundamentals of EEG measurement Measurement Science Review ${\bf 2}$ 1–11
- Thut G et al 2017 Guiding transcranial brain stimulation by EEG/ MEG to interact with ongoing brain activity and associated functions: a position paper Clinical Neurophysiology 128 843–57
- Thut G, Schyns P G and Gross J 2011 Entrainment of perceptually relevant brain oscillations by non-invasive rhythmic stimulation of the human brain *Frontiers in Psychology* 2 170

- Traikapi A and Konstantinou N 2021 Gamma oscillations in Alzheimer's disease and their potential therapeutic role *Frontiers in Systems Neuroscience* 15 782399 (https://frontiersin.org/articles/10.3389/fnsys.2021.782399)
- Violante I R and Okyere P 2024 Can neurotechnology revolutionize cognitive enhancement? *PLoS Biol.* 22 e3002831
- Wang D, Marcantoni E, Clouter A, Shapiro K L and Hanslmayr S 2024 Rhythmic sensory stimulation as a noninvasive tool to study plasticity mechanisms in human episodic memory Current Opinion in Behavioral Sciences 58 101412
- Wasserstein R L and Lazar N A 2020 ASA statement on statistical significance and p-values *The Theory of Statistics in Psychology* ed C W Gruber (Springer International Publishing) 1–10 (10.1007/978-3-030-48043-1_1)
- Zhang S, Cui H, Li Y, Chen X, Gao X and Guan C 2024 Improving SSVEP-BCI performance through repetitive anodal tDCS-based neuromodulation: insights from fractal EEG and brain functional connectivity *IEEE Trans. Neural Syst. Rehabil.* Eng. 32 1647–56